

## Supporting Information

### **Ni–P codoping engineered MoS<sub>2</sub> basal planes for electrocatalytic water splitting: Insights from density functional theory**

Le Thanh Phuong,<sup>a</sup> Sampath Prabhakaran,<sup>\*c</sup> Do Hwan Kim,<sup>\*,a,b</sup>

<sup>a</sup>Graduate School of Integrated Energy-AI, Jeonbuk National University, Jeonju, Jeonbuk 54896, Republic of Korea

<sup>b</sup>Division of Science Education, Graduate School of Department of Energy Storage/Conversion Engineering (BK21 Four), Jeonbuk National University, Jeonju, Jeonbuk 54896, Republic of Korea. (orcid.org/0000-0002-2976-6873)

<sup>c</sup>Department of Nano Convergence Engineering, Jeonbuk National University, Jeonju, Jeonbuk 54896, Republic of Korea (orcid.org/0000-0003-1568-7864)

\*Corresponding: E-mail: spkaran10@jbnu.ac.kr, dhk201@jbnu.ac.kr.

## DFT Calculations

### *d*-band center

Norskov et al. formulated the *d*-band center theory, whereby the *d*-band center is considered a characteristic indicator of catalytic activity. This principle has been utilized to anticipate the reactivity of metals, as confirmed by Hammer and Norskov in 1995<sup>1</sup>.

To determine the positions of the *p*- and *d*-band centers, we used the following equation:

$$\varepsilon = \frac{\int_{-\infty}^{\infty} E\rho(E)dE}{\int_{-\infty}^{\infty} \rho(E)dE}, \quad (1)$$

where  $\rho$  is the *d*-band density,  $E$  is the *d*-band energy, and  $\rho dE$  is the number of states.

### HER

$\Delta G_{H^*}$  is calculated using the CHE method as follows<sup>2</sup>:

$$\Delta G_{H^*} = \Delta E_{H^*} + \Delta E_{ZPE} - T\Delta S_H, \quad (2)$$

where:

$\Delta E_{H^*}$  = total energy for hydrogen adsorption obtained from DFT calculations;

$\Delta E_{ZPE}$  = change in zero-point energy of hydrogen between the adsorbed state and gas phase; and

$\Delta S_H$  = difference in entropy between the adsorbed and gas-phase hydrogen at room temperature (T = 298.15 K).

The adsorption energy is calculated as follows:

$$\Delta E_{H^*} = E_{substrate + adsorbent} - E_{substrate} - E_{adsorbent}, \quad (3)$$

where:

$E_{substrate + adsorbent}$  = ground-state energy of the substrate adsorbent;

$E_{substrate}$  = ground-state energy of the substrate; and

$E_{adsorbent}$  = ground-state energy of the adsorbent.

The intermediate stage of  $H_{\text{ads}}$ , as described by the Volmer and Heyrovsky reactions, is as follows <sup>3</sup>:

Volmer reaction for hydrogen adsorption is expressed as:



Heyrovsky reaction for molecular hydrogen formation:



Tafel-expressed HER <sup>4</sup> :



The HER catalytic activity is commonly assessed by analyzing the variations in the  $\Delta G_{*H}$  value during the Volmer step (Equation 4), which is a crucial aspect of the HER process <sup>5, 6, 7</sup>.

## OER

The oxidation performance of the anode in the water-splitting process was evaluated by examining the OER using the methodology established by Nørskov et al. <sup>8,9</sup>.

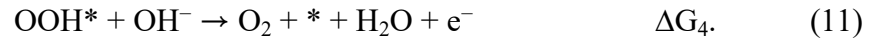
The overall OER can be summarized as follows:



$*OH$ ,  $*O$ , and  $*OOH$  denote the intermediate species formed upon the adsorption of oxygen species onto the active sites of the catalyst;  $G_1$ ,  $\Delta G_2$ ,  $\Delta G_3$ , and  $\Delta G_4$  represent  $\Delta G$  in each step.

OER involves  $4e^-$  in alkaline media:





The  $\Delta G$  in reaction steps (Eqs. (8–11)) was determined as follows:

$$\Delta G = \Delta E + \Delta_{\text{ZPE}} - T\Delta S - neU + \Delta G(\text{pH}), \quad (12)$$

where:

$\Delta E$  = adsorption energy with oxygen species;

$\Delta_{\text{ZPE}}$  = changes in zero-point energy;

$\Delta S$  = changes in entropy;

$T$  = temperature under standard conditions (298.15 K,  $p = 1$  bar);

$-neU$  = correct bias in electron transfer with  $-neU$  as the electrode potential; and

$\Delta G(\text{pH}) = \Delta kT \ln[\text{H}^+]$ ; correct free energy based on the  $\text{H}^+$  ion concentration.

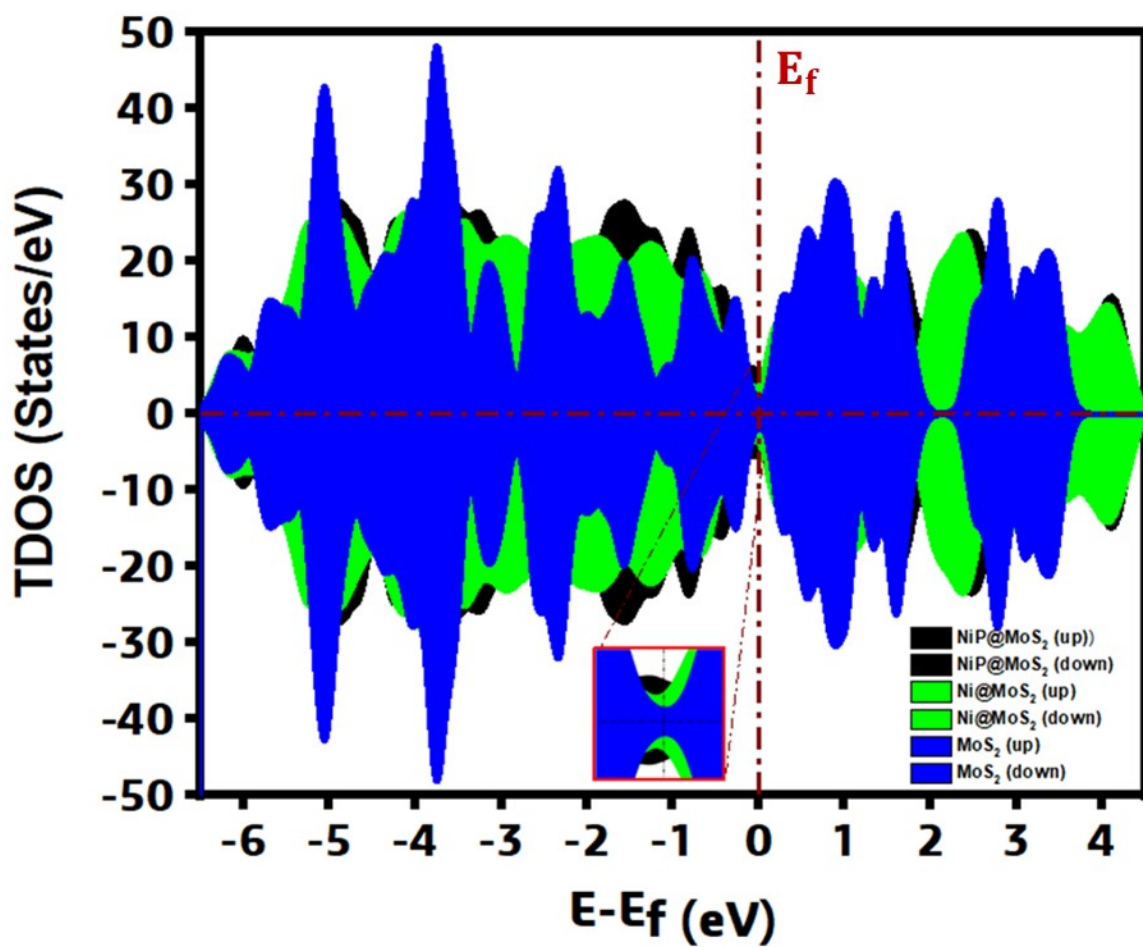


**Figure S1.** Calculated spin-polarized total density of states for the 1T'-phase NiP@MoS<sub>2</sub>, Ni@MoS<sub>2</sub>, and MoS<sub>2</sub>, with respect to the stable crystalline structures.

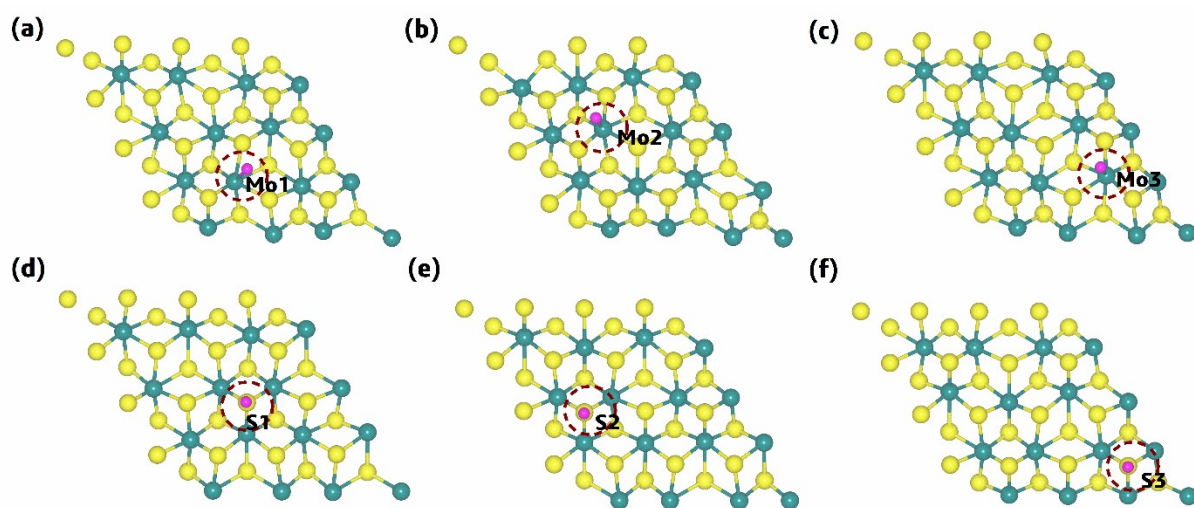


**Figure S2.** Top view of the  $^*H$  intermediate adsorbed on different active sites of the 1T phase  $MoS_2$ , (a–c) Mo and (d–f) S. Green, yellow, and pink colors represent the Mo, S, and H atoms, respectively.

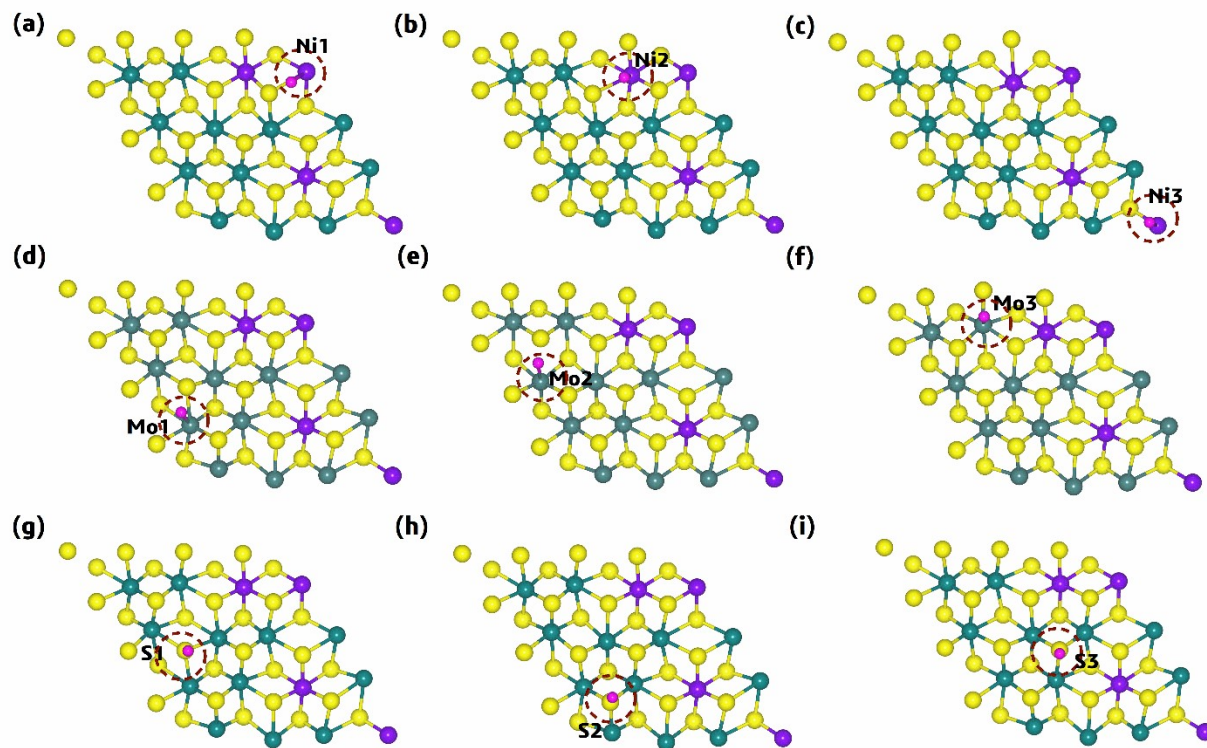


**Figure S3.** Top view of the  $^*H$  intermediate adsorbed on different active sites of the 1T phase of Ni@MoS<sub>2</sub>: (a–c) Ni, (d–f) Mo, and (g–i) S. Green, yellow, purple, and pink colors represent the Mo, S, Ni, and H atoms, respectively.

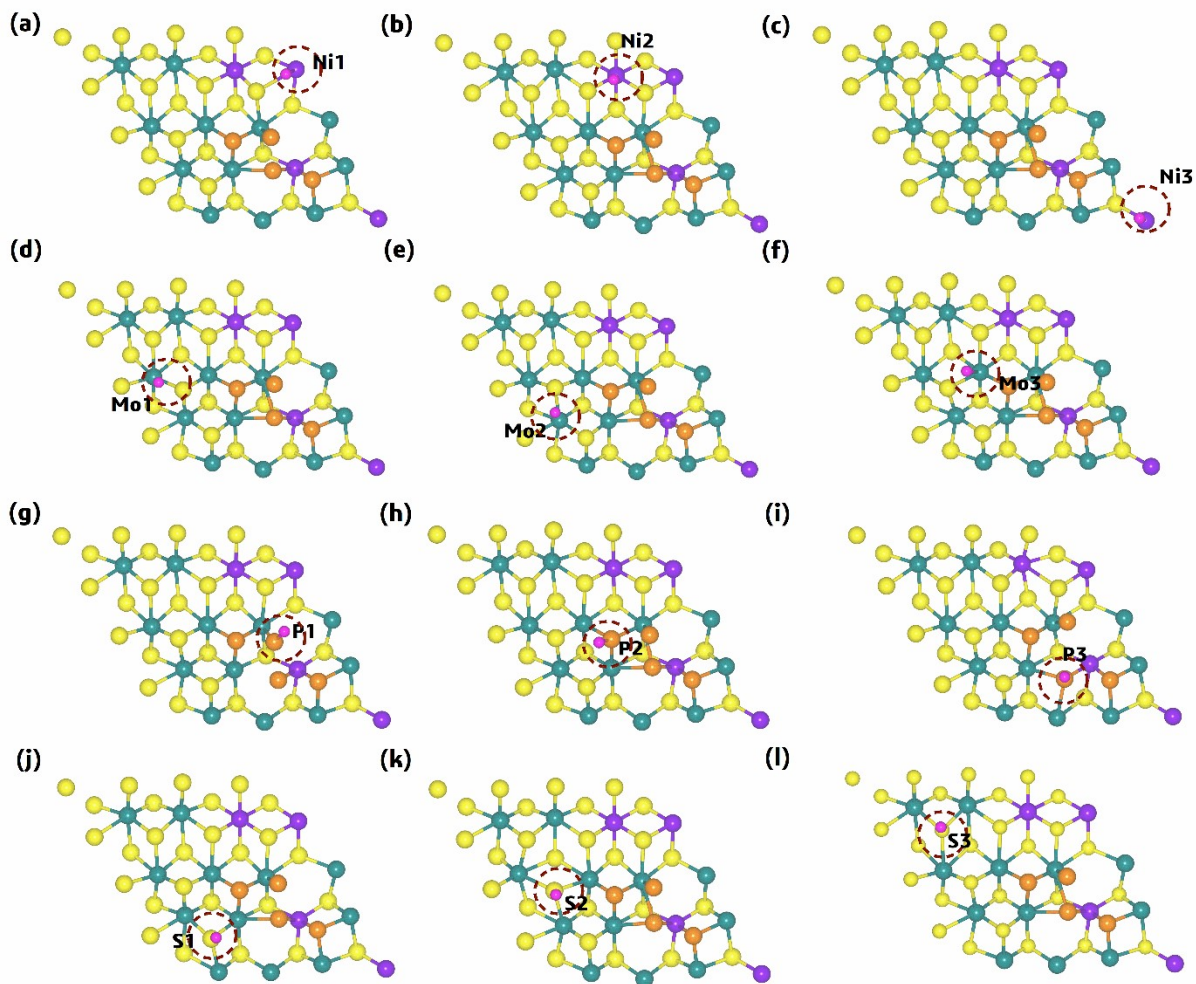


**Figure S4.** Top view of the  $^*H$  intermediate adsorbed on different active sites of the 1T phase of NiP@MoS<sub>2</sub>: (a–c) Ni, (d–f) Mo, (g–i) P, and, (j–l) S. Green, yellow, purple, orange, and pink colors represent the Mo, S, Ni, P, and H atoms, respectively.

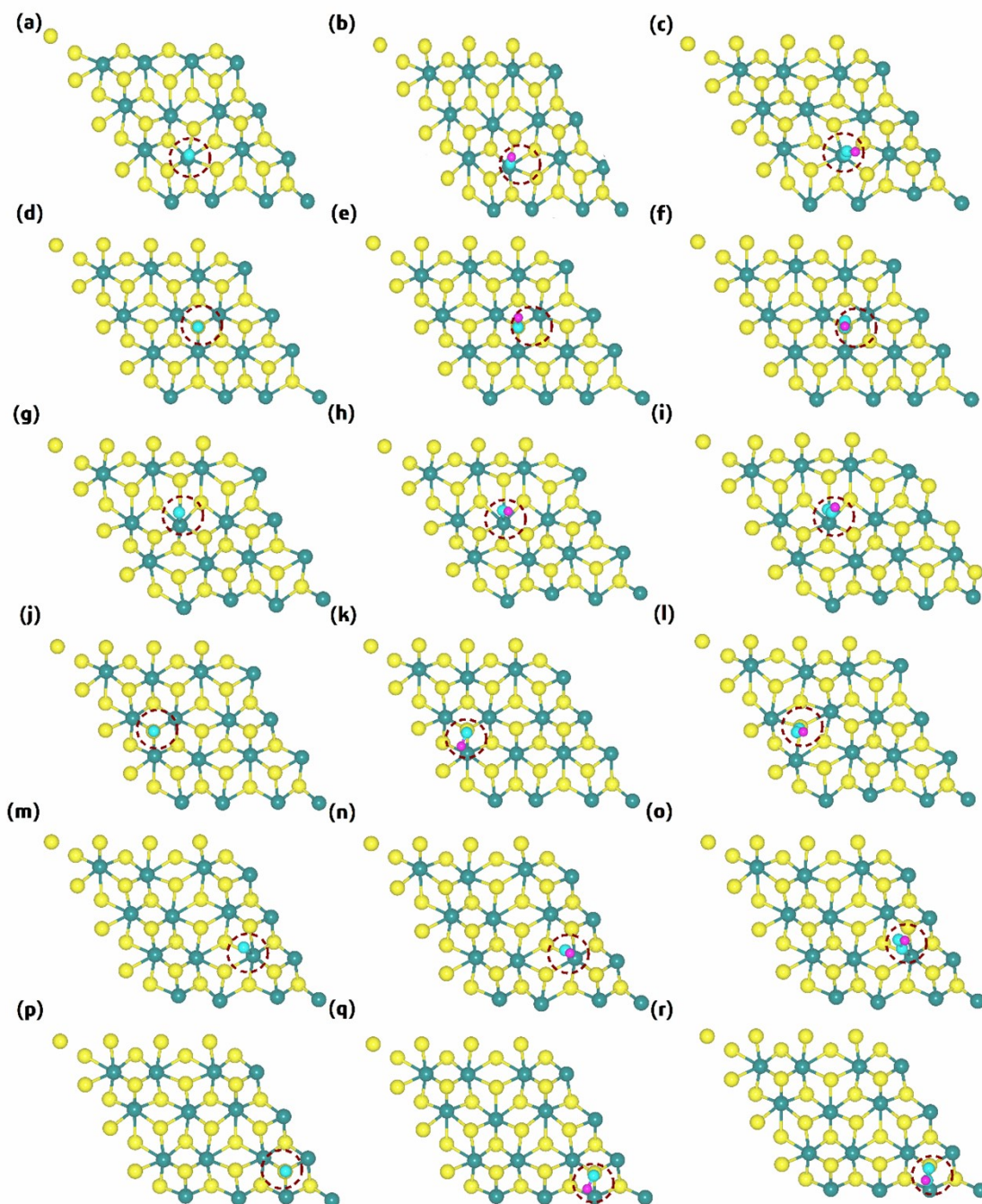


**Figure S5.** Top view of the OER intermediates (\*O, \*OH, and \*OOH) adsorbed on different active sites of the 1T phase of MoS<sub>2</sub>: (a–c) Mo1, (d–f) S1, (g–i) Mo2, (j–l) S2, and (m–o) Mo3, and (p–r) S3. Green, yellow, pink, and cyan colors represent the Mo, S, H, and O atoms, respectively.

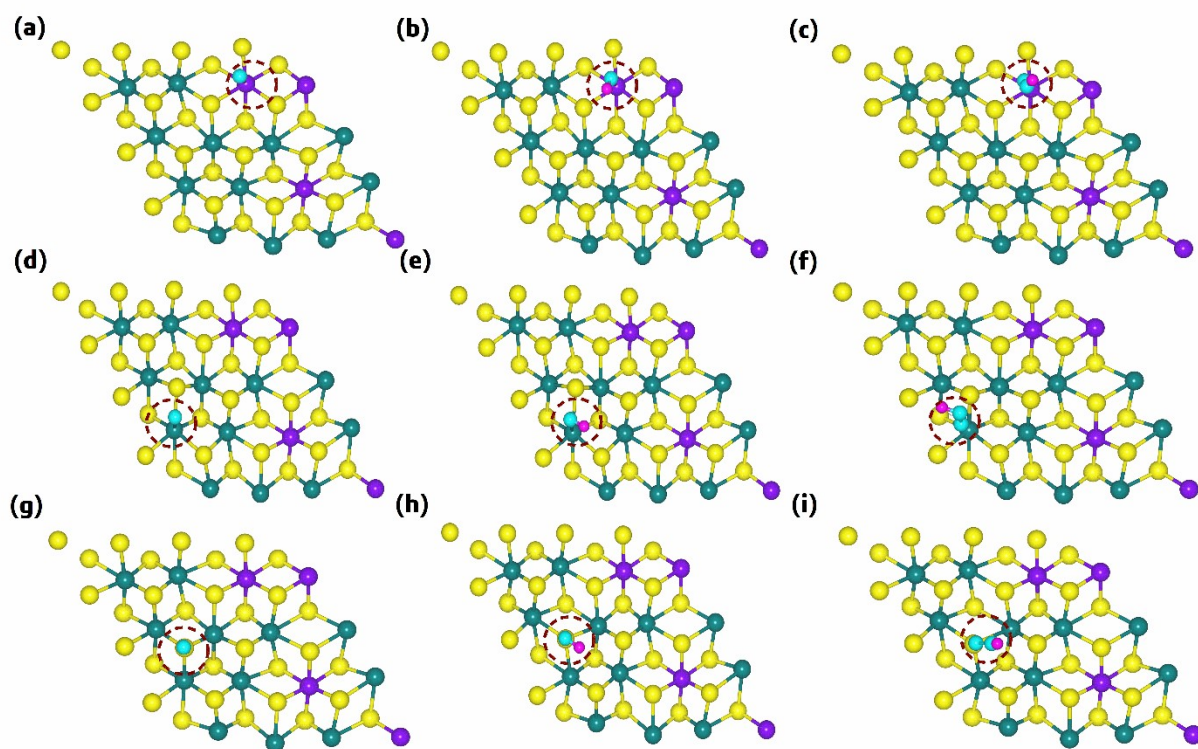


**Figure S6.** Top view of the OER intermediates ( $^*O$ ,  $^*OH$ , and  $^*OOH$ ) adsorbed on different active sites of the 1T phase of Ni@MoS<sub>2</sub>: (a–c) Ni1, (d–f) Mo1, and (g–i) S1. Green, yellow, purple, pink, and cyan colors represent the Mo, S, Ni, H, and O atoms, respectively.

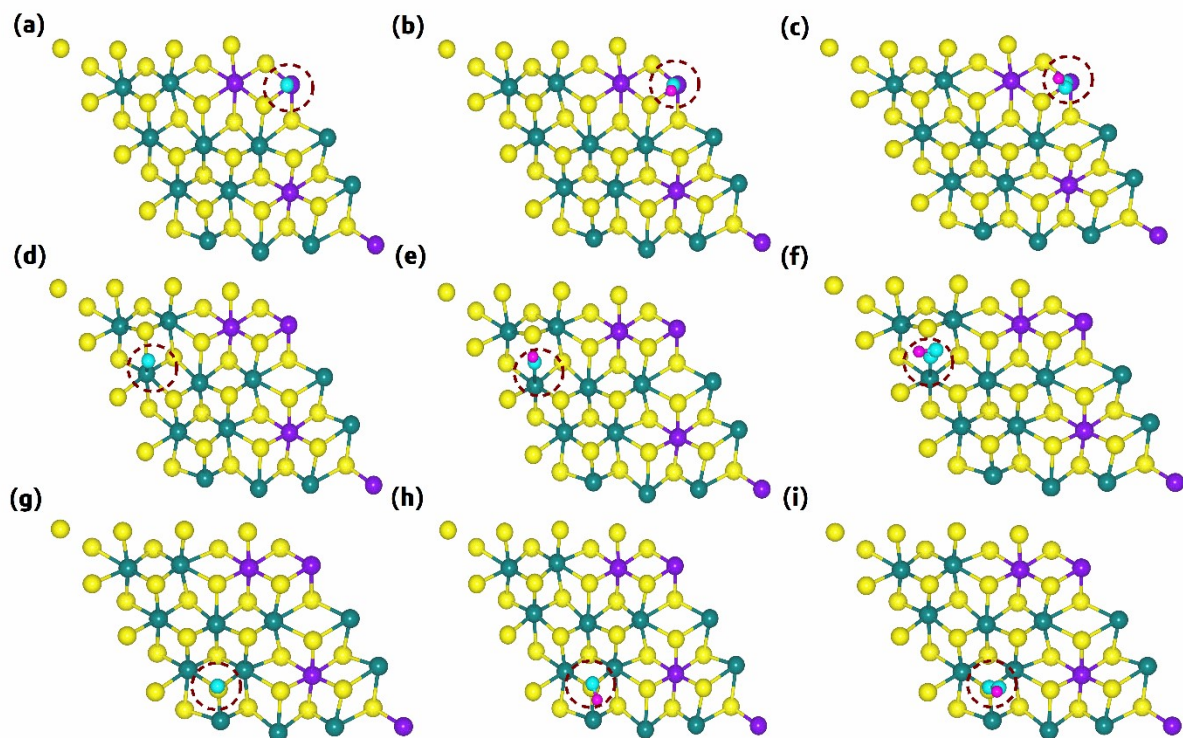


**Figure S7.** Top view of the OER intermediates ( $^*O$ ,  $^*OH$ , and  $^*OOH$ ) adsorbed on different active sites of the 1T phase of Ni@MoS<sub>2</sub>: (a–c) Ni<sub>2</sub>, (d–f) Mo<sub>2</sub>, and (g–i) S<sub>2</sub>. Green, yellow, purple, pink, and cyan colors represent the Mo, S, Ni, H, and O atoms, respectively.

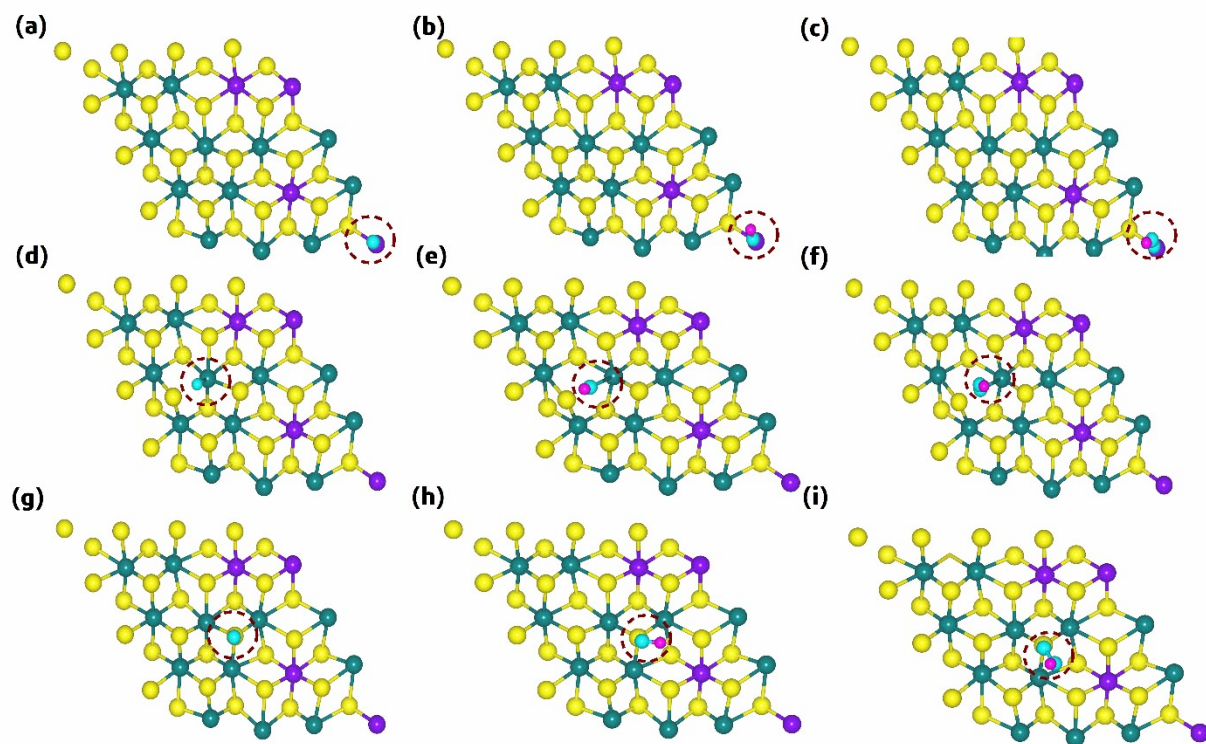


**Figure S8.** Top view of the OER intermediates ( $^*O$ ,  $^*OH$ , and  $^*OOH$ ) adsorbed on different active sites of 1T phase of Ni@MoS<sub>2</sub>: (a–c) Ni<sub>3</sub>, (d–f) Mo<sub>3</sub>, and (g–i) S<sub>3</sub>. Green, yellow, purple, orange, pink, and cyan colors represent the Mo, S, Ni, P, H, and O atoms, respectively.

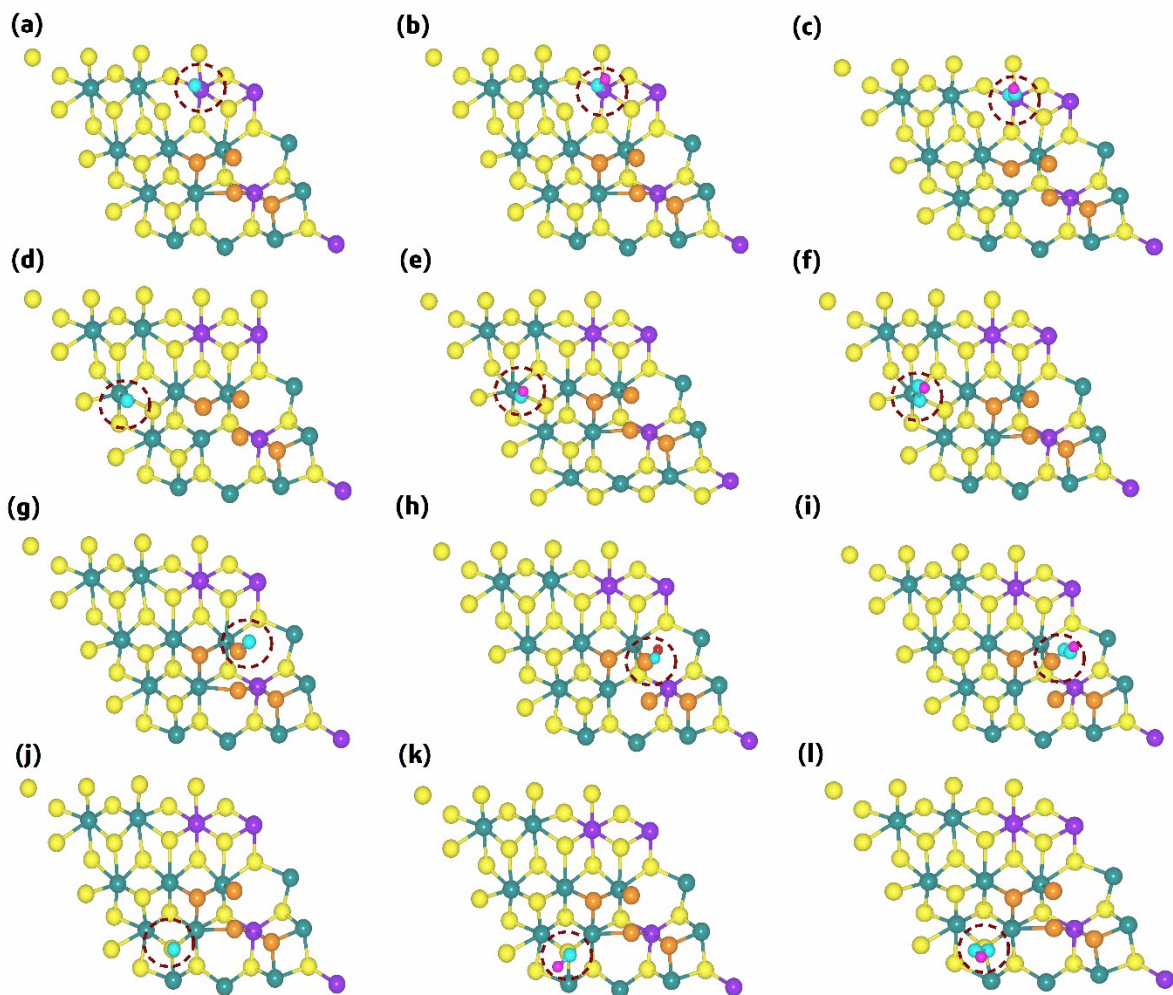


**Figure S9.** Top view of the OER intermediates ( $^*O$ ,  $^*OH$ , and  $^*OOH$ ) adsorbed on the different active sites of 1T phase of  $NiP@MoS_2$ : (a–c) Ni1, (d–f) Mo1, (g–i) P1, and (j–l) S1. Green, yellow, purple, orange, pink, and cyan colors represent the Mo, S, Ni, P, H, and O atoms, respectively.

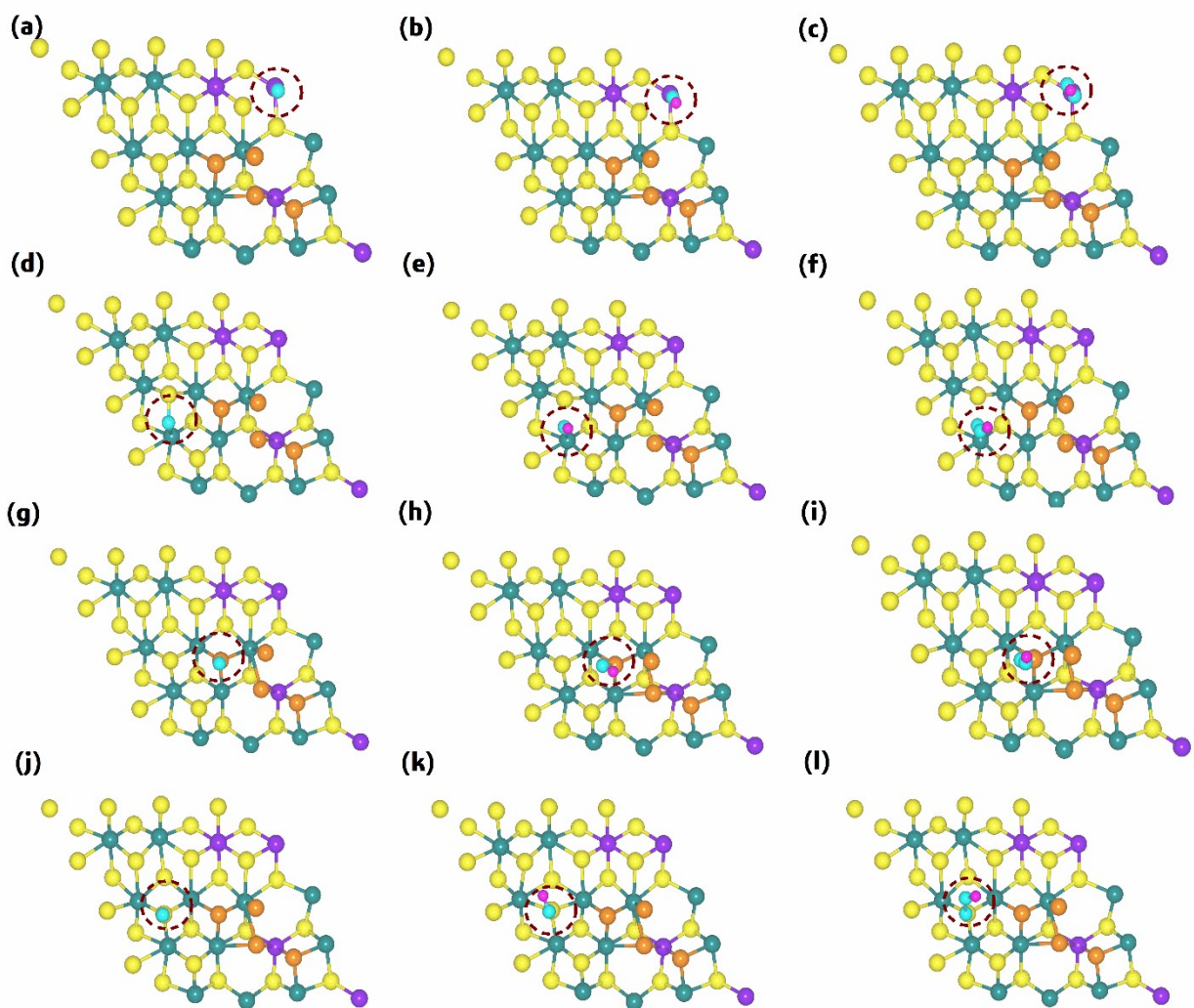


**Figure S10.** Top view of the OER intermediates (\*O, \*OH, and \*OOH) adsorbed on the different active sites of 1T phase of NiP@MoS<sub>2</sub>: (a–c) Ni<sub>2</sub>, (d–f) Mo<sub>2</sub>, (g–i) P<sub>2</sub>, and (j–l) S<sub>2</sub>. Green, yellow, purple, orange, pink, and cyan colors represent the Mo, S, Ni, P, H, and O atoms, respectively.

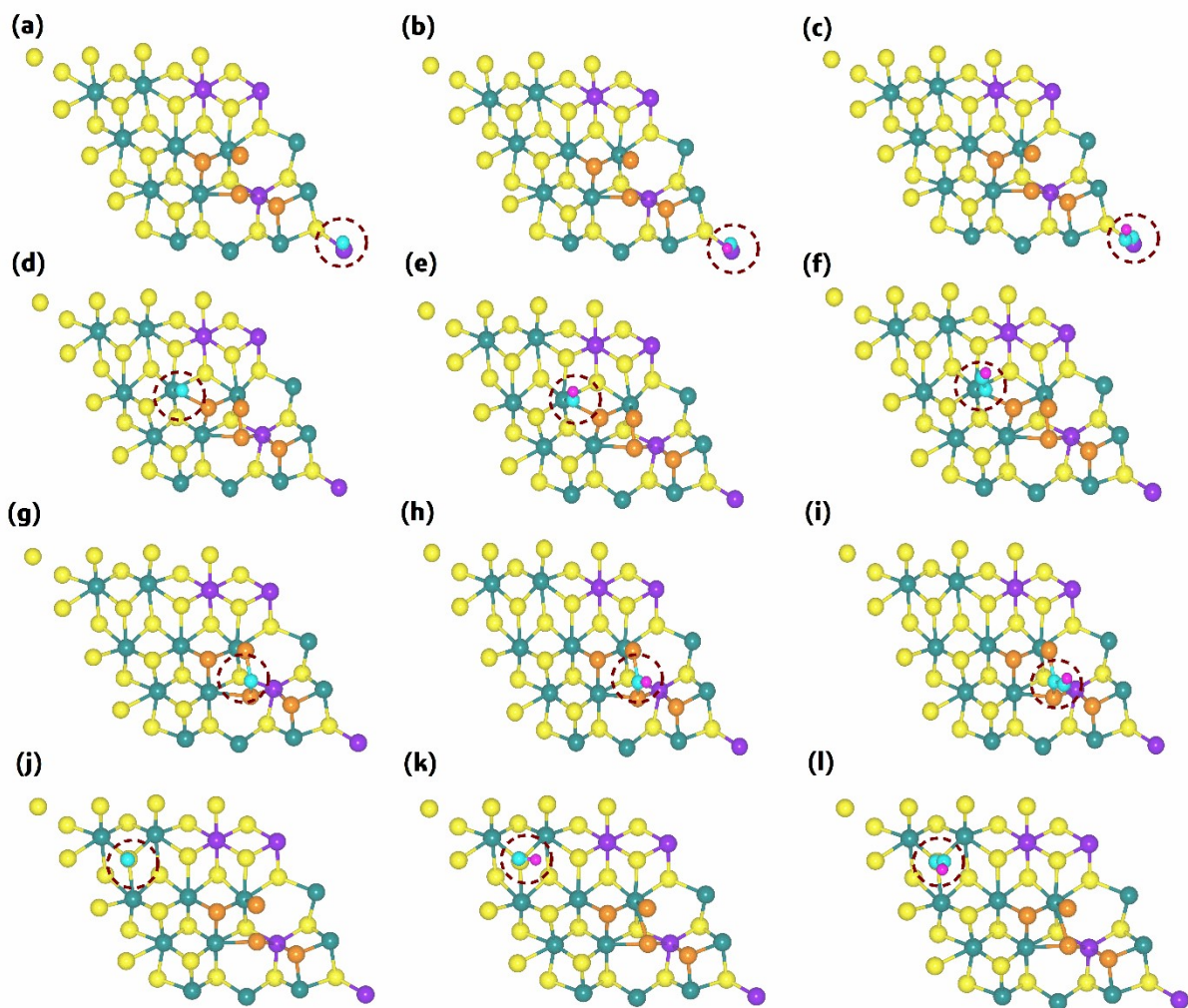


**Figure S11.** Top view of the OER intermediates ( $^*O$ ,  $^*OH$ , and  $^*OOH$ ) adsorbed on different active sites of the 1T phase of NiP@MoS<sub>2</sub>: (a–c) Ni<sub>3</sub>, (d–f) Mo<sub>3</sub>, (g–i) P<sub>3</sub>, and (j–l) S<sub>3</sub>. Green, yellow, purple, orange, pink, and cyan colors represent the Mo, S, Ni, P, H, and O atoms, respectively.

**Table S1** Calculated  $\Delta G$  and  $\eta$  of different active sites for various catalysts.

| Catalyst             | Active sites | $\Delta G$ (eV) |              |              |              | $\eta_{\text{OER}}$ (V) |             |
|----------------------|--------------|-----------------|--------------|--------------|--------------|-------------------------|-------------|
|                      |              | $\Delta G_1$    | $\Delta G_2$ | $\Delta G_3$ | $\Delta G_4$ |                         |             |
| MoS <sub>2</sub>     | Mo           | 1               | 3.112        | 0.682        | 2.565        | -1.439                  | 1.88        |
|                      |              | 2               | 3.022        | 0.222        | 3.404        | -1.728                  | 2.17        |
|                      |              | 3               | 2.632        | 0.612        | 3.405        | -1.729                  | 2.18        |
|                      | S            | 1               | 2.797        | 0.403        | 2.863        | -1.143                  | 1.63        |
|                      |              | 2               | 2.750        | 1.409        | 1.942        | -1.184                  | 1.52        |
|                      |              | 3               | 3.022        | 0.142        | 3.677        | -1.922                  | 2.45        |
| Ni@MoS <sub>2</sub>  | Ni           | 1               | 1.613        | 0.829        | 0.657        | 1.820                   | 0.59        |
|                      |              | 2               | 1.916        | 0.185        | 2.397        | 0.422                   | 1.17        |
|                      |              | 3               | 2.269        | 0.692        | 1.432        | 0.527                   | 1.04        |
|                      | Mo           | 1               | 2.104        | 0.158        | 3.166        | -0.508                  | 1.94        |
|                      |              | 2               | 2.051        | 0.832        | 2.430        | -0.393                  | 1.20        |
|                      |              | 3               | 2.019        | 0.579        | 2.751        | -0.429                  | 1.52        |
|                      | S            | 1               | 1.919        | 1.804        | 0.875        | 0.323                   | 0.69        |
|                      |              | 2               | 1.409        | 2.337        | 1.573        | -0.399                  | 1.11        |
|                      |              | 3               | 1.435        | 2.325        | 1.970        | -0.810                  | 1.10        |
| NiP@MoS <sub>2</sub> | Ni           | 1               | 2.585        | 1.128        | 2.627        | -1.419                  | 1.40        |
|                      |              | 2               | 1.569        | 1.722        | 3.152        | -1.523                  | 1.92        |
|                      |              | 3               | 2.757        | 0.812        | 2.381        | -1.030                  | 1.53        |
|                      | Mo           | 1               | 2.569        | 0.722        | 3.289        | -1.660                  | 2.06        |
|                      |              | 2               | 2.669        | 1.177        | 2.597        | -1.523                  | 1.44        |
|                      |              | 3               | 2.808        | 0.737        | 2.924        | -1.549                  | 1.69        |
|                      | P            | 1               | 1.996        | 1.065        | 2.074        | -1.215                  | 0.84        |
|                      |              | 2               | 1.897        | 1.342        | 2.575        | -0.894                  | 1.35        |
|                      |              | 3               | 1.621        | 1.252        | 1.210        | 0.837                   | <b>0.39</b> |
| S                    | 1            | 2.372           | 1.013        | 2.279        | -0.745       | 1.14                    |             |
|                      | 2            | 2.134           | 1.729        | 1.894        | -0.837       | 0.90                    |             |
|                      | 3            | 1.967           | 1.596        | 2.094        | -0.737       | 0.86                    |             |

## References

1. B. Hammer and J. K. Nørskov, *Nature*, 1995, 376, 238-240.
2. J. K. Nørskov, T. Bligaard, A. Logadottir, J. Kitchin, J. G. Chen, S. Pandalov and U. Stimming, *Journal of The Electrochemical Society*, 2005, 152, J23.
3. V. Kichigin and A. Shein, *Electrochimica Acta*, 2016, 201, 233-239.
4. E. Skúlason, V. Tripkovic, M. E. Björketun, S. Gudmundsdóttir, G. Karlberg, J. Rossmeisl, T. Bligaard, H. Jónsson and J. K. Nørskov, *The Journal of Physical Chemistry C*, 2010, 114, 18182-18197.
5. C. Ling, L. Shi, Y. Ouyang and J. Wang, *Chemistry of Materials*, 2016, 28, 9026-9032.
6. G. Gao, A. P. O'Mullane and A. Du, *Acs Catalysis*, 2017, 7, 494-500.
7. D. Er, H. Ye, N. C. Frey, H. Kumar, J. Lou and V. B. Shenoy, *Nano letters*, 2018, 18, 3943-3949.
8. N. Li, Y. Nam and J. Y. Lee, *Applied Surface Science*, 2020, 514, 146073.
9. J. K. Nørskov, J. Rossmeisl, A. Logadottir, L. Lindqvist, J. R. Kitchin, T. Bligaard and H. Jónsson, *The Journal of Physical Chemistry B*, 2004, 108, 17886-17892.